K^+-dependent paradoxical membrane depolarization and Na^+ overload, major and reversible contributors to weakness by ion channel leaks

Karin Jurkat-Rott[a,1], Marc-André Weber[b], Michael Fauler[a], Xiu-Hai Guo[a,2], Boris D. Holzherr[a], Agathe Paczulla[a], Nikolai Nordsborg[a], Wolfgang Joechle[c], and Frank Lehmann-Horn[a,1]

[a]Institute of Applied Physiology, Ulm University, Ulm, Germany; [b]Department of Diagnostic and Interventional Radiology, Heidelberg University Hospital, Heidelberg, Germany; and [c]Department of Clinical Chemistry, Ulm University Hospital, Ulm, Germany

Edited by Erwin Neher, Max Planck Institute for Biophysical Chemistry, Goettingen, Germany, and approved January 12, 2009 (received for review November 6, 2008)

Normal resting potential (P1) of myofibers follows the Nernst equation, exhibiting about −85 mV at a normal extracellular K^+ concentration ($[K^+]_o$) of 4 mM. Hyperpolarization occurs with decreased $[K^+]_o$, although at $[K^+]_o$ < 1.0 mM, myofibers paradoxically depolarize to a second stable potential of −60 mV (P2). In rat myofiber bundles, P2 also was found at more physiological $[K^+]_o$ and was associated with inexcitability. To increase the relative frequency of P2 to 50%, $[K^+]_o$ needed to be lowered to 1.5 mM. In the presence of the ionophore gramicidin, $[K^+]_o$ reduction to only 2.5 mM yielded the same effect. Acetazolamide normalized this increased frequency of P2 fibers. The findings mimic hypokalemic periodic paralysis (HypoPP), a channelopathy characterized by hypokalemia-induced weakness. Of myofibers from 7 HypoPP patients, up to 25% were in P2 at a $[K^+]_o$ of 4 mM, in accordance with their permanent weakness, and up to 99% were in P2 at a $[K^+]_o$ of 1.5 mM, in accordance with their paralytic attacks. Of 36 HypoPP patients, 25 had permanent weakness and myoplasmic intracellular Na^+ ($[Na^+]_i$) overload (up to 24 mM) as shown by in vivo ^{23}Na-MRI. Acetazolamide normalized $[Na^+]_i$ and increased muscle strength. HypoPP myofibers showed a nonselective cation leak of 12–19.5 μS/cm^2, which may explain the Na^+ overload. The leak sensitizes myofibers to reduced serum K^+, and the resulting membrane depolarization causes the weakness. We postulate that the principle of paradoxical depolarization and loss of function upon $[K^+]_o$ reduction may apply to other tissues, such as heart or brain, when they become leaky (e.g., because of ischemia).

amphotericin B | gramicidin | hypokalemic periodic paralysis | membrane potential | muscle weakness

Hypokalemic periodic paralysis (HypoPP) presents as recurrent episodes of generalized flaccid weakness triggered by carbohydrate-induced hypokalemia or exposure to cold (1). The progressive weakness that occasionally is described has been explained by a structural myopathy with vacuoles and T-tubular aggregates (2). The hypokalemia-induced weakness was explained by the in vitro depolarization of myofiber membranes to −55 mV in a 1-mM K^+ solution (3, 4). At physiological extracellular K^+ concentrations ($[K^+]_o$), the myofibers were depolarized only slightly, a finding that is in accordance with normal muscle strength between episodes (3, 4).

In muscle, $[K^+]_o$ reduction diminishes currents with hyperpolarizing effects, such as the outward component of the inwardly rectifying K^+ (Kir) channels (5). Therefore, in contrast to hyperpolarization predicted by the Nernst equation, a higher K^+ gradient obtained by low $[K^+]_o$ may cause paradoxical depolarization (5). The hyperpolarizing outward Kir current decreases with depolarization, and this decrease may progress until the activation of other outward K^+ currents stabilizes the membrane potential at a second, less negative value. Therefore, muscle fibers may equilibrate to 1 of 2 putative stable potentials, leading to a bimodal distribution of the membrane potential (E_m). Basically, this distribution would be expected under all $[K^+]_o$ conditions if the Kir current is counterbalanced by depolarizing inward currents.

It has been shown that HypoPP is caused by mutations in 2 voltage-gated cation channels in the skeletal muscle, Cav1.1 and Nav1.4 (6, 7). The Cav1.1 Ca^{2+} channels are essential for excitation−contraction coupling, and all voltage sensor mutations cause HypoPP-1 (6). The Nav1.4 Na^+ channels generate action potentials, and mutations in the voltage sensors of domains 2 and 3 cause the clinically similar, but less common, HypoPP-2 (7, 8). The effects of the mutations on channel pore currents suggest reduced function, but they are not able to explain satisfactorily the association with hypokalemia (9). Recently, a mutation-induced cation leak through an aberrant pore that is open at the resting potential was described (10, 11). Such a cation leak that causes a gain of function of the mutant channel may counteract the Kir current and increase the tendency of the muscle fiber membrane to depolarize (12). For the leak to cause episodes of weakness, the paradoxical depolarization must occur at serum K^+ levels considerably higher than the experimentally used level of 1 mM, a $[K^+]_o$ that is too low to be compatible with life.

A nonselective cation leak also would lead to a permanent inward Na^+ current. Increased intracellular Na^+ ($[Na^+]_i$) should activate the Na/K-ATPase and, thereby, be extruded from the cell. However, according to results in neurons, the Na/K-ATPase may not be able to compensate a permanent inward Na^+ current (13). Myoplasmic Na^+ overload has been suggested to be myotoxic (14), and the resulting myopathic changes could be much more severe than just vacuoles or T-tubular aggregates. We tested whether a cation leak leads to a permanent $[Na^+]_i$ overload of pathogenetic relevance.

Our study contains 2 parts. The first is an examination of $[Na^+]_i$ overload and muscle weakness as clinical signs of a pathologic cation leak in the model disorder HypoPP. Thirty-six patients volunteered for the study, all of whom were examined by new ^{23}Na MRI (15). Seven of the patients consented to muscle biopsy to measure K^+-dependent membrane potential distribution and leaks. The electrical properties of Kir currents also were studied in human controls. The second part of the study examines the K^+ paradox in rat muscle treated with the Na^+ ionophore gramicidin (GD) (16) to simulate the leak present in HypoPP.

Author contributions: K.J.-R., M.-A.W., and F.L.-H. designed research; M.-A.W., M.F., X.-H.G., B.D.H., A.P., N.N., and W.J. performed research; K.J.-R., M.-A.W., M.F., X.-H.G., B.D.H., N.N., and W.J. analyzed data; and K.J.-R. and F.L.-H. wrote the paper.

The authors declare no conflict of interest.

This article is a PNAS Direct Submission.

Freely available online through the PNAS open access option.

[1]To whom correspondence may be addressed. E-mail: karin.jurkat-rott@uni-ulm.de or frank.lehmann-horn@uni-ulm.de.

[2]Permanent address: Department of Neurology, Xuanwu Hospital, Beijing, China.

This article contains supporting information online at www.pnas.org/cgi/content/full/0811277106/DCSupplemental.

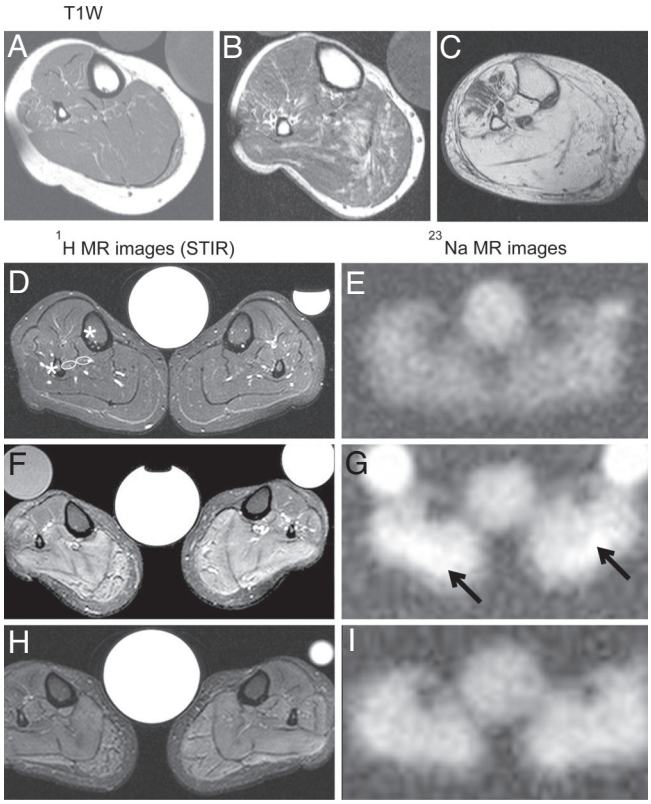

Fig. 1. ^{1}H and ^{23}Na measurements in the calf muscles of HypoPP patients. (*A–C*) Axial T1-weighted MR images from 3 related Cav1.1-R1239H patients: a 35-year-old woman (*A*), her 55-year-old uncle (*B*), and her 80-year-old grandmother whose limb muscles were predominantly replaced with fat (*C*). (*D–I*) T2-weighted STIR ^{1}H (*Left*) and ^{23}Na-MR images (*Right*) from a healthy control (*D* and *E*) and a 37-year-old patient (*F–I*), the sister of the patient in *A*. The images in *F* and *G* were taken before treatment, and the images in *H* and *I* were taken after treatment with 250 mg/d AZ for 4 weeks. Note the very high hydrogen intensities in the STIR sequence (*F*) and the elevated Na^+ concentration before treatment (*G*, arrows indicate highest Na signal intensities) and their improvement after treatment. The central reference contains 0.3% NaCl solution; occasional side tubes containing 0.3% NaCl in 1% agarose (*Left*) and 0.6% NaCl in H_2O (*Right*) were additional standards.

Results

Permanent Weakness and Fatty Muscle Degeneration in HypoPP. Of the 36 patients diagnosed with HypoPP according to clinical criteria (1), 28 had a Cav1.1 mutation (HypoPP-1): R528H in 13 patients, R528G in 1 patient, R1239H in 12 patients, and R1239G in 2 patients. Eight patients had a Nav1.4 mutation (HypoPP-2): R672H in 3 patients, R672G in 2 patients, and R675Q in 3 patients. On average, patients who had the R1239H had the most frequent episodes (up to daily), whereas those harboring the R528H mutation had monthly episodes, and HypoPP-2 patients had yearly episodes. All R1239H patients and half of all other patients presented with permanent muscle weakness of varying degrees, including wheelchair dependence [supporting information (SI) Table S1]. Of the 25 patients with permanent weakness, 21 displayed fatty muscle degeneration, and 18 displayed edema in a ^{1}H-MRI of the lower legs. The degree of fatty muscle degeneration increased with age (Fig. 1 *A–C*).

The degree of hypokalemia-induced weakness was measured before and after provocation with 2 g of glucose per kilogram body weight and 15 U/l insulin (Table 1, lines 1 and 2). Paralysis occurred with severe hypokalemia in HypoPP-2 and Cav1.1-R528H/G patients and with moderate hypokalemia in Cav1.1-R1239H/G patients. In contrast, controls remained in the normokalemic range and did not display any weakness.

Intracellular Na^+ Overload and Muscle Weakness. ^{23}Na-MRI and ^{1}H-MRI and an assessment of muscle strength according to the Medical Research Council of Great Britain (MRC) scale (17) were performed on all 36 patients (Fig. 1 *D–G*). At rest, ^{23}Na-MRI revealed markedly higher $[Na^+]_i$ in weak muscles than in strong muscles (Fig. 2; Table 1, lines 3 and 4), although weak muscles tend to have fatty degeneration, and fat exhibits a lower Na^+ concentration than muscle. The ^{1}H-MRI showed that the $[Na^+]_i$ overload was accompanied by water in the form of edema (Table 1, line 5). The correlation between water content and Na^+ yielded a linear coefficient of determination (R^2) of 0.63. The ^{23}Na-MRI and ankle torque before and after cooling were measured on 31 of the 36 patients. Local cooling increased the ^{23}Na and ^{1}H signal intensities and weakness in all HypoPP patients but not in controls (Table 1, lines 6 and 7). The correlation between Na^+ accumulation and muscle strength reduction was linear ($R^2 = 0.70$).

Of the severely affected HypoPP-1 patients, 6 were administered acetazolamide (AZ), 250 mg/d, and K^+, 60 mmol/d, for 4 weeks. The treatment reduced $[Na^+]_o$ by 21.9% ± 5.2% ($P < 0.001$) and increased ankle torque by 32.9% ± 12.8% ($P < 0.001$). The association between the increase in muscle strength and myoplasmic Na^+ reduction followed the same linear correlation observed with cooling.

Semiquantitative Real-Time PCR of Na/K-ATPase cDNA. A permanent Na^+ gradient shift may affect Na/K-ATPase expression. The cDNA for the 3 major muscle ATPase subunits from 8 HypoPP samples and 6 controls were examined by semiquantitative real-time PCR. The ratio of target transcript concentration (ATP1A1, ATPA1A2, or ATP1B1) to reference transcript concentration (ACTB) was calculated using external standard curves (*SI Methods*, Fig. S1 and Table S2). For the α1 and β1 transcripts, no significant differences were found between the patient and control samples (2.9 ± 2.5 vs. 2.1 ± 1.6 for ATP1A1; 0.9 ± 0.3 vs. 0.9 ± 0.2 for ATP1B1), but there was a significant reduction in ATP1A2 transcripts (0.5 ± 0.2 vs. 1.3 ± 0.6, $P = 0.011$).

Bimodal Distribution of Resting Potentials and the K^+ Paradox. Muscle fiber bundles were obtained from 3 healthy controls and 7 HypoPP patients harboring either a Nav1.4 mutation (R672H, R672G, or R675Q) or a Cav1.1 mutation (R528H in 1 patient; R1239H in 3 patients). Normal muscle fibers revealed 2 stable E_m in 4-mM K^+: the well-polarized potential P1 (−83 mV) in 95% of fibers and a depolarized potential P2 (−61 mV) in 5% of fibers (Table 1, line 8). The HypoPP fibers had a P1 of −74 mV to −77 mV in 76% to 91% of fibers, depending on the mutation, and a P2 of −58 mV to −61 mV in 9% to 24% of fibers (Table 1, line 8; Fig. 3*A*). Normal and HypoPP muscle fibers with an $E_m \leq -59$ mV were unable to generate an action potential (Fig. 3*B*), suggesting that the permanent weakness in HypoPP patients may be attributed to a fraction of unexcitable fibers. In 1.5-mM K^+, 87% of normal fibers belonged to the P1 fraction (−99 mV), and 13% belonged to the P2 fraction (−61 mV; Table 1, line 9). In contrast, 83% to 99% of HypoPP fibers were related to P2 (−54 mV to −64 mV) at 1.5-mM K^+ (Table 1, line 9), a finding that is in agreement with the idea that membrane depolarization at low K^+ is responsible for episodes of hypokalemic paralysis.

Role of Kir Channels in E_m and Putative Cation Leaks in HypoPP-1. The depolarization indicates that there must be an imbalance between the inward cation leak and outward Kir current. Therefore, both Kir current and leak were examined in excised human muscle fibers. Current density–voltage relationships in normal myofibers were measured to determine the characteristics of Kir channel conductance. To eliminate superimposing currents, the solution contained

Table 1. Overview of in vivo and in vitro measurements

L	Parameter	Nav1.4-R672H/G Nav1.4-R675Q	Cav1.1-R528H/G	Cav1.1-R1239H/G	Controls
Serum K^+ (mM) before and after glucose/insulin provocation					
1	Before	4.2 ± 0.3 [4] $P = 0.74$	4.1 ± 0.2 [6] $P = 0.18$	4.1 ± 0.4 [6] $P = 0.33$	4.3 ± 0.2 [7]
2	After	2.3 ± 0.4 [4] $P < 0.001$	2.0 ± 0.3 [6] $P < 0.001$	2.6 ± 0.3 [6] $P < 0.001$	3.6 ± 0.3 [7]
In vivo values					
3	Calf strength (MRC)	5 [8]	5 [14]	4 [14]	5 [12]
4	Myoplasmic Na^+ (mM)	19.0 ± 3.2 [8] $P < 0.001$	18.2 ± 3.2 [14] $P = 0.04$	24.7 ± 3.4 [14] <0.001	15.0 ± 1.4 [12]
5	Relative ^1H signal (−)	20.3 ± 8.8 [8] $P = 0.05$	23.6 ± 6.8 [14] $P = 0.02$	38.4 ± 9.0 [14] <0.001	19.3 ± 3.3 [12]
Cooling-induced changes					
6	Torque reduction (%)	15.6 ± 8.5 [7] $P < 0.01$	19.8 ± 7.5 [11] $P < 0.01$	22.9 ± 11.8 [14] $P < 0.01$	0.0 ± 0.0 [7]
7	^{23}Na increase (%)	5.0 ± 5.1 [5] $P = 0.09$	14.9 ± 9.9 [11] $P < 0.001$	10.20 ± 9.1 [14] $P = 0.01$	0.4 ± 2.9 [7]
In vitro resting membrane potentials (E_m)					
8	E_m (mV) at 4 mM K^+	85% −77 ± 6 [3]	91% −75 ± 5 [1]	76% −74 ± 5 [3]	95% −83 ± 5 [3]
		15% −60 ± 2 [128]*	9% −61 ± 2 [76]*	24% −58 ± 3 [128]*	5% −61 ± 2 [369]*
9	E_m (mV) at 1.5 mM K^+	2% −76 ± 2 [3]	17% −80 ± 7 [1]	1% −72 ± 1 [3]	87% −99 ± 3 [3]
		98% −64 ± 9 [41]*	83% −59 ± 6 [36]*	99% −54 ± 4 [91]*	13% −61 ± 4 [127]*

L = line, [] indicate number of individuals, []* indicate number of fibers. Values are mean ± SD except values in line 3, which are median. The *t* tests were two-sided, unpaired for comparing patients and controls ($P < 0.001$) for the E_m values in the upper rows of lines 8 and 9.

TTX but not Cl^-. The Kir conductance in 4-mM K^+ was 10-fold greater, and the relationship was steeper, than in 1-mM K^+ (Fig. 4). Nevertheless, at potentials of approximately −75 mV, both curves were flat and even showed a negative resistance, a prerequisite for a rapid shift to P2.

To determine if a putative cation leak current is induced by Cav1.1 voltage sensor mutations, the membrane currents of 3 HypoPP-1 patients and 3 controls were compared. The resulting current densities for Cav1.1-R528H and -R1239H fibers were significantly larger than for controls ($P < 0.01$ at ≥ −80 mV; Fig. 4). The subtraction of the control currents from HypoPP currents can be assumed to yield the mutation-related leak current. The conductance determined for the linear hyperpolarization was 12.0 $\mu S/cm^2$ for Cav1.1-R528H and 19.5 $\mu S/cm^2$ for -R1239H.

Role of the Cation Leak in E_m and Intracellular Na^+. The E_m of rat diaphragm muscle strips was measured in K^+ solutions at concentrations between 0 and 6 mM. In all experiments, at all K^+ concentrations, and in both control and gramicidin (GD) solutions, 2 stable potentials were observed according to a bimodal distribution. On average, 0.1 μM GD in 4 mM K^+ shifted P1 from −78.0 ± 0.49 mV to −74.0 ± 0.46 mV ($P < 0.001$), whereas P2 was unchanged at approximately −60 mV. However, the most striking effect was that the presence of the ionophore changed the relative frequencies of P1 and P2. The plot of the P1 relative frequency (well-polarized stable potential) versus $[K^+]_o$ was best fitted by a log-normal cumulative distribution function (Boltzmann-like relationship). In the $[K^+]_o$ range of 0–6 mM, the ratio of P1:P2 frequencies were inverted in controls, from 4:1 to 1:4. The turning point, equal P1 and P2 frequencies of 0.5, was at 1.6 mM K^+ for controls and 2.4 mM K^+ for GD; GD therefore shifted the curve to the right (Fig. 5).

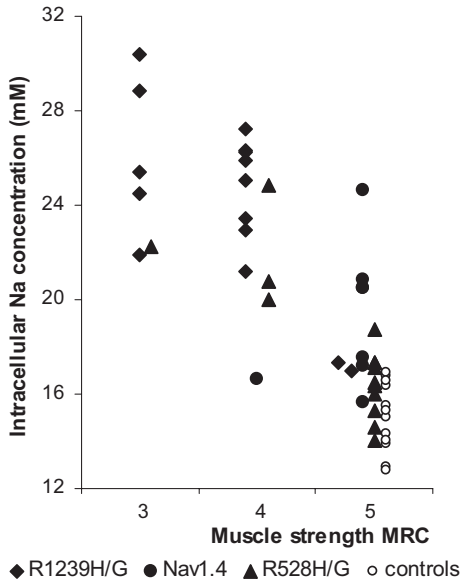

Fig. 2. Correlation of strength and $[Na^+]_i$ in 36 HypoPP patients. The $[Na^+]_i$ values obtained with a ^{23}Na-MRI of the lower legs and the values of plantar flexor muscle strength measured according to the MRC grading scale (*closed symbols*) show a clear correlation. Values from 12 healthy controls are shown as open circles.

The addition of 100 μM AZ to GD shifted the curve back to the left and increased the relative frequency for P1 in low-K^+ solutions (Fig. 5*B*). Because the addition of AZ generally enhanced hyperpolarization, most likely by opening several types of K^+ channels, such as BK channels (18, 19), the turning point is not at a P1 frequency of 0.5 but rather at 0.65. The turning point corresponds to a 1.5-mM $[K^+]_o$, similar to that of controls, suggesting that the ratio of total K^+ conductance to total cation and leak conductance is restored by AZ. To demonstrate that the effect of AZ is valid for cation leaks in general and is not the result of some sort of interaction of AZ with GD, we repeated the experiments with a structurally very different Na^+ ionophore, amphotericin B (AmB), known not to interact with AZ (20). Two stable potentials also were observed in fibers incubated in 10 μM AmB. AmB shifted the turning point of the Boltzmann-like relationship to the right, to 2.9 mM K^+, compared with 1.6 mM K^+ for controls (Fig. 5*B*). The addition of 100 μM AZ to the AmB solution shifted the curve back to the left and increased the relative frequency for P1 in low-K^+ solutions, just as did the addition of GD (Fig. 5*B*). Again, AZ caused hyperpolarization, and the turning point at the P1 frequency at 0.65 corresponded to 1.5 mM K^+.

In dose–response experiments (not shown), the EC_{50} was determined to be 0.55 μM GD in a 4-mM $[K^+]_o$ and 0.03 μM GD in a 2.5-mM $[K^+]_o$. These results suggest that smaller leaks resulting from a lower GD concentration require a larger K^+ reduction to increase the P2 relative frequency to the same degree.

To confirm the hypothesis that $[Na^+]_i$ overload in patients is caused by a cation leak, muscular $[Na^+]_i$ was measured in rat muscle strips using atomic absorption spectroscopy. In 4-mM K^+, the application of 0.1 μM GD significantly increased the

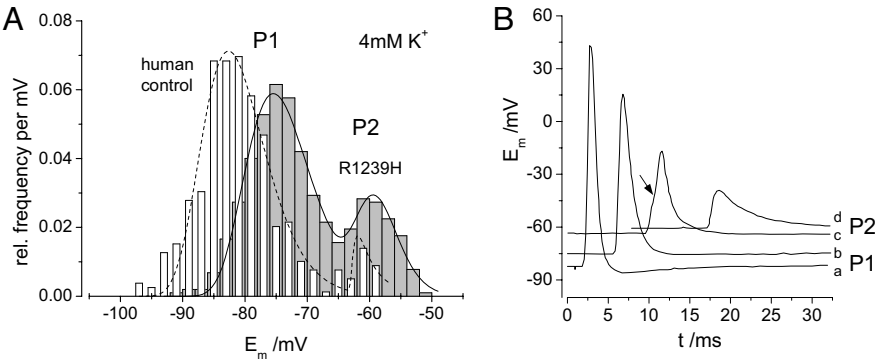

Fig. 3. Resting (E_m) and action potentials of normal and HypoPP fibers. (*A*) Bimodal distribution of E_m of human control fibers (white, $n = 369$) and R1239H-HypoPP muscle fibers (gray, $n = 128$) in 4-mM K^+. HypoPP fibers have an increased probability for the second stable membrane potential of −60 mV (P2); the first stable membrane potential (P1) in HypoPP fibers is depolarized by ≈ 10 mV compared with the controls. (*B*) Action potentials (AP) in the endplate region elicited from various holding potentials of −82 mV (*a*), −75 mV (*b*), −62 mV (*c*), and −59 mV (*d*). At *c* there is a minimal AP beginning at the arrow; at *d* there is no AP, only the endplate potential.

Na^+ concentration from 18.4 ± 4.9 mM ($n = 11$) to 25.7 ± 6.9 mM ($n = 18$; $P < 0.01$).

Twitch measurements revealed a decrease in force during the stepwise reduction of K^+ in both control and GD solutions (Fig. 5*C*). The K^+ dependence was similar to that of the membrane potentials. A force reduction of 30% occurred in the control solution in 1-mM K^+ and in the GD solution in 2.5-mM K^+, showing that leaky fibers require a smaller K^+ reduction to lose force. Compared with the large P2 population, the reduction in force in the presence of GD was milder, because most of the depolarized fibers did not exceed −58 mV and still were excitable.

Discussion

This study shows that (*i*) cation leaks depolarize myofibers in a $[K^+]_o$-dependent manner; (*ii*) leaks shift the Boltzmann-like relationship of the paradoxical depolarization to physiological $[K^+]_o$ values so that large leaks can cause weakness at normal $[K^+]_o$; (*iii*) leak-induced depolarization is associated with $[Na^+]_i$ overload and edema; (*iv*) AZ can normalize $[Na^+]_i$ in vivo, repolarize myofibers, and increase force; and (*v*) ^{23}Na-MRI is a valuable method for the diagnosis, treatment, follow-up, and prognosis of HypoPP and other disorders with an $[Na^+]_i$ overload.

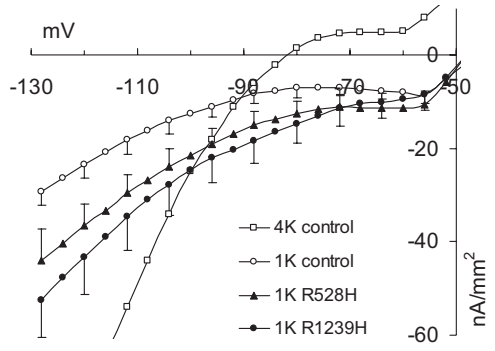

Fig. 4. Kir conductance and cation leak in human myofibers. Steady-state current density–voltage relationships were determined in 1.0-mM K^+ for 7 normal myofibers (1K control) and 4 (1K R528H) and 5 myofibers (1K R1239H) from patients. The difference between the curves for patients and controls corresponds to the mutation-related leak current. In addition, 8 normal myofibers (4K control) were measured in 4.0-mM K^+. Note that the 4K curve is much steeper ($g_{max} = 261$ μS/cm^2 at hyperpolarization) than the 1K curve ($g_{max} = 26.5$ μS/cm^2) of the control fibers according to the higher Kir conductance in 4-mM K^+. To avoid superimposing currents, the solutions contained TTX, not Cl^-.

Reducing $[K^+]_o$ diminishes hyperpolarizing currents such as rectifying K^+ currents. Therefore, reducing $[K^+]_o$ causes a paradoxical depolarization in control muscle at $[K^+]_o$ less than 1 mM (5). Accordingly, a loss of K^+ rectifier channel function causes weakness such as that found, for example, in Andersen syndrome (21). Our measurements of human control muscle in a $[K^+]_o$ of 1 mM show a 90% reduction in Kir conductance compared with a $[K^+]_o$ of 4 mM; this reduction is comparable to the Kir channel blocking caused by Ba^{2+} (22).

The E_m can be approximated by considering only 2 current types, the hyperpolarizing rectifying K^+ current and the depolarizing nonselective cation inward current (12, 22). The E_m equals the voltage at which these 2 currents have the same absolute value. Therefore, primary depolarization, such as that found in HypoPP, can indicate an imbalance between these 2 currents, particularly an increase of the inward current, as suggested by our measurements in HypoPP-1 patients and previous reports on HypoPP-2 (10, 11).

The observed bimodal E_m distribution cannot be caused by fast- and slow-twitch fibers because the rat diaphragm has only 1 fiber type, intermediate. Variability in specimen quality also is unlikely to be the cause, because the distributions were consistent in many preparations. Therefore, the bimodal E_m distribution reflects the existence of 2 stable membrane potentials (5). A leak increases the inward cation current, favoring P2 and, thus, a likelihood of depolarization beyond −60 mV because of action potential failure. Although P1 seems to follow the Nernst equation, P2 is somewhat stable over all conditions and probably results from the activation of an additional K^+ conductance that electrically stabilizes the membrane at P2 in a manner such as that seen with non-inactivating voltage-gated K^+ channels.

A nonselective cation leak leads to Na^+ overload in vitro and in vivo. Possible compensatory overexpression of the Na/K-ATPase may be expected; however, quantitative RT-PCR suggests that the opposite, a reduction in the $\alpha 2$ subunit, occurs, similar to the functional decrease in leaky neurons (13). The reduced ATPase expression is similar to that of the K-depleted rat model of HypoPP (23). Reduced ATPase may indicate that serum K^+ levels need to be maintained by limiting transport into cells. As a result, both Na and K gradients should be reduced, as indicated by our finding of a $[Na]_i$ overload.

We conclude that HypoPP may be caused by nonselective cation leaks. The HypoPP mutations associated with more severe HypoPP phenotypes, such as Cav1.1-R1239H/G with up to daily paralytic episodes, generate relatively large leaks (≈ 19.5 μS/cm^2). These large leaks explain the greater P2 frequency with more common permanent weakness at normal $[K^+]_o$ in all R1239H/G patients and the higher resting $[Na^+]_i$ with fatty myopathy in 11 of 14 patients.

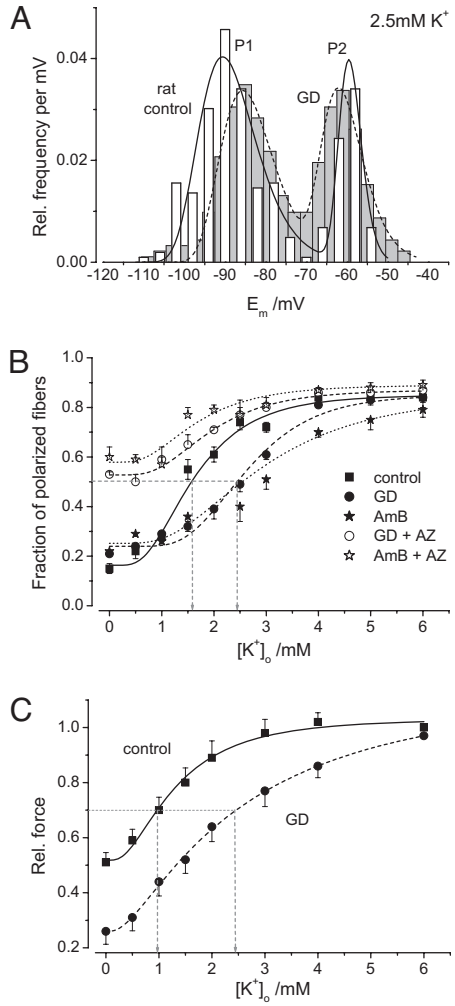

Fig. 5. Resting potentials (E_m) of rat muscle strips treated with GD. (*A*) Bimodal distribution of E_m in control (white, $n = 257$ fibers) and rat diaphragm strips treated with 0.1 μM GD (gray, $n = 265$ fibers) to create leaks. As in HypoPP, the relative frequency of the second stable potential (P2) at −60 mV increased, and the first stable potential (P1) was depolarized by ≈ 5 mV for the leaky fibers. (*B*) Relative P1 frequency dependent on external K^+. Fitting the data points (6–7 strips each) to a multimodal log-normal probability density function enabled comparison. The turning point is at 2.5 mM K^+ in GD-treated leaky fibers, at 2.9 mM in AmB-treated fibers, and at 1.5 mM for controls, suggesting that the leaky fibers have a higher probability for the second stable potential (P2 = −60 mV) when $[K^+]_o$ decreases. The addition of 100 μM AZ to the leaky fibers resulted in the restoration of the fraction of polarized fibers, particularly in low K^+. (*C*) Dependence of twitch force on $[K^+]_o$ (5 strips at each data point). The force reduction in GD-treated muscles and control muscles upon $[K^+]_o$ reduction reflects the loss of polarized fibers illustrated in *B*.

Therefore, in agreement with earlier clinical recommendations (24), AZ therapy to repolarize muscle (e.g., by opening BK channels (18, 19) and lowering $[Na^+]_i$) may improve permanent weakness in these patients. In other words, permanent weakness in HypoPP may be caused by a gain of function of the mutant channels rather than by disturbed muscle structure. However, $[Na^+]_i$ overload caused by the leak may contribute to a disturbed structure on the long term. The tight association between $[Na^+]_i$ and weakness ($R^2 = 0.7$) may indicate that, as in Duchenne muscular dystrophy, Na^+ overload can be myotoxic (14) and contribute to fatty myopathy (25). Therefore, it is reasonable to assume that AZ may delay the fatty replacement of muscle tissue in HypoPP. Monitoring $[Na^+]_i$ with ^{23}Na-MRI may prove useful for therapy follow-up. If unavailable, conventional ^{1}H-MRI can be used instead because of the relatively high correlation of edema to $[Na^+]_i$ ($R^2 = 0.63$).

The HypoPP mutations associated with milder phenotypes, such as Cav1.1-R528H with monthly episodes, generate smaller leaks (≈ 12 μS/cm^2). Smaller GD leaks had an EC_{50} at a lower $[K^+]_o$ than larger leaks, a finding that explains the relatively severe hypokalemia during episodes, the smaller $[Na^+]_i$ increase, and the relative rarity of fatty myopathy. During episodes, however, these patients may be at a higher risk for hypokalemic complications, such as cardiac arrest. In our 36 families with R528H and 27 families with R1239H, ictal deaths occurred in 15 individuals who had R528H (at a median age of 22 years), indicating the importance of ictal K^+ intake and the avoidance of triggers promoting hypokalemia, such as insulin secretion caused by carbohydrate-rich meals.

The principle of paradoxical depolarization upon serum K^+ reduction that underlies HypoPP pathogenesis may apply to all tissues equipped with Kir channels, including the brain, heart, muscle, kidney, and leukocytes (22, 26, 27). In particular, paradoxical depolarization and loss of function may arise when these tissues become leaky (e.g., because of ischemia, hypertrophy, hormones, or drugs) (28–30) or exhibit $[Na^+]_i$ overload (14). Serum K^+ values in the lower-normal range therefore should be avoided, as demonstrated by the first clinical studies in which continuous K^+ supplementation was proven to be beneficial in hypertensive and postinfarction states (31).

Methods

Participants. The study was approved by the institutional review boards in Heidelberg and Ulm and was conducted according to the Declaration of Helsinki. Patients were diagnosed as having permanent weakness if their MRC grading was less than 5 at 2 different examinations (0 = complete paralysis; 5 = full strength) (17). Isometric ankle torque at the maximal voluntary activation of the ankle dorsiflexors was recorded with an aluminum-frame device that holds the participant's leg securely. Force was measured by a strain gauge (KM38, ME-MESysteme); its output was digitized (MiniDigi 1A, Axon Instruments). The system was used for torque measurements before and after cooling and treatment. The relative changes are given as a percentage. For the cooling test, bags of ice water were wrapped around 1 lower leg for 30 min to enable a comparison with the unprovoked leg. Mutations were detected by the direct sequencing of genomic DNA (6, 7).

MRI. The T2 decay of the Na signal is bi-exponential with a much faster component for intracellular Na than for extracellular Na because the high density of intracellular protein reduces the mobility of Na. An ultra-short echo time (TE) below 0.5 ms is required (15). The ^{23}Na signal was recorded from the lower legs (Fig. 1 *E*, *G*, and *I*), and 3D-radial images were analyzed in regions of interest (ROI) located on the soleus muscle and in a control tube with 160 pixels containing a 0.3% NaCl solution. The pulse sequence was T1-weighted (TE = 0.2 ms) and highlighted intracellular Na (15). A much higher concentration (51 mM) of the NaCl reference solution corresponding to the extracellular solution was required to obtain signal intensities similar to those of normal intracellular Na (15 mM) (Fig. 1*G*). On average, the Na signal intensity of control muscle was 0.864 compared with the signal of the 0.3% NaCl solution (15). Because $[Na^+]_i$ is 15 mM, according to physiology books, the control signal of 0.864 was set to 15 mM, and the Na^+ of HypoPP muscles was determined by linear extrapolation.

Muscular water content was measured with ^{1}H-MRI using a standard T1-weighted spin-echo sequence and a fat-suppressed T2-weighted short tau inversion recovery (STIR) sequence to differentiate between edema and fatty replacement. The signals were normalized to background. Muscle edema was defined as an area of elevated signal intensity in the STIR sequence. Two experienced radiologists determined ROI by consensus. For both ^{23}Na and ^{1}H broadband measurements, a unique double-resonant birdcage coil was used (Rapid Biomed).

Functional in Vitro Studies. ***Preparations.*** Human muscle specimens > 3.5 cm in length were removed from the quadriceps of 7 patients and 3 controls, all of whom had given informed consent. The specimens were divided into bundles 2 mm in diameter and were allowed to reseal for at least 2 h. Because the availability of human muscle is limited, rat muscle was used for systematic experiments on the effects of K^+ variation on membrane potential in the presence of a membrane leak. Sixty-day-old Wistar rats were killed by CO_2 asphyxiation, and their diaphragms were removed and divided into several strips.

Solutions. The control solution contained 108 mM NaCl, 4 mM KCl, 1.5 mM $CaCl_2$, 0.7 mM $MgSO_4$, 26.2 mM $NaHCO_3$, 1.7 mM NaH_2PO_4, 9.6 mM Na-gluconate, 5.5 mM glucose, and 7.6 mM sucrose and was 290 mosmol/l at 37 °C. The pH was adjusted to 7.4 by gassing with 95% O_2 and 5% CO_2. For leak measurements with 3 microelectrodes, Cl^- was replaced with the membrane-impermeant methanesulfonate, and 1 μM TTX was added. GD (0.1 μM) and AmB (10 μM) were used as ionophores for monovalent cations. AZ (100 μM) (Sigma) was added where indicated.

Twitch force was measured by a force transducer (FT03, Grass Instrument Co.) at optimal length. The bundles were stimulated supramaximally with 1-ms pulses.

Resting membrane potentials. Histograms of the potentials were smoothed by density estimation. The potentials exhibited a 2-peak distribution of polarized and depolarized fibers displayed as probability density. A multimodal log-normal probability density function was fitted to the data, and the fraction of polarized fibers was plotted against $[K^+]_o$. The concentration response curves were fitted to the measured potentials according to fdf = fdf_{min}+ (fdf_{max} − fdf_{min})/(1 + 10^((logEC_{50} − [GD])p)) with fdf as the fraction of depolarized fibers, fdf_{max} and fdf_{min} as the maximum and minimum effects, and p as the Hill coefficient. The median effective EC_{50} values were calculated from these fits.

Current–voltage relationships. Three microelectrodes (5−15 MΩ) were inserted at the approximate midlength of a fiber (3). The voltage of the central electrode was fed to a voltage-clamp amplifier and altered in 4-mV steps by rectangular pulses of 80-ms duration. Membrane current densities were calculated using the steady-state values at the 2 voltage and current electrodes. Pooled values were plotted with standard deviations.

Action potentials. The recording electrode was implanted next to the endplate. Using a second microelectrode, a constant current was injected to yield various holding potentials. A sucking electrode stimulated the nerve ending.

Intracellular Na^+ concentration. Rat muscles were exposed to the solution of interest for 15 min, washed in an isotonic sucrose solution for 5 min, and dried at 100 °C overnight to a constant weight. After cooling to room temperature, the dried muscles were weighed (20–80 mg). The addition of 1 ml nitric acid dissolved the muscles overnight. Aliquots of the solution were measured with an atomic spectrometer in emission mode (Perkin-Elmer AAS1100). Aliquots of certified reference material were used as controls (NCS ZC81001 pork muscle, expiring 2010, LGC Promochem). The certified reference values were 0.2% for Na^+.

ACKNOWLEDGMENTS. We are grateful to Dr. S. Nielles-Vallespin and A. Nagel for their contribution to ^{23}Na-MRI, Dr. R. Rüdel and Dr. B. Böhm for helpful discussions, and E. Schoch for force measurements. This work was supported by grant JU470/1–2 from the German Research Foundation (DFG).

1. Venance SL, *et al.* (2006) The primary periodic paralyses: Diagnosis, pathogenesis and treatment. *Brain* 129:8–17.
2. Links TP, Zwarts MJ, Wilmink JT, Molenaar WM, Oosterhuis HJ (1990) Permanent muscle weakness in familial hypokalaemic periodic paralysis. Clinical, radiological and pathological aspects. *Brain* 113:1873–1889.
3. Rüdel R, Lehmann-Horn F, Ricker K, Küther G (1984) Hypokalemic periodic paralysis: In vitro investigation of muscle fiber membrane parameters. *Muscle Nerve* 7:110–120.
4. Ruff RL (1999) Insulin acts in hypokalemic periodic paralysis by reducing inward rectifier K^+ current. *Neurology* 53:1556–1563.
5. Geukes Foppen RJ, van Mil HG, van Heukelom JS (2002) Effects of chloride transport on bistable behaviour of the membrane potential in mouse skeletal muscle. *J Physiol* 542:181–191.
6. Jurkat-Rott K, *et al.* (1994) A calcium channel mutation causing hypokalemic periodic paralysis. *Hum Mol Genet* 3:1415–1419.
7. Jurkat-Rott K, *et al.* (2000) Voltage-sensor sodium channel mutations cause hypokalemic periodic paralysis type 2 by enhanced inactivation and reduced current. *Proc Natl Acad Sci USA* 97:9549–9554.
8. Sternberg D, *et al.* (2001) Hypokalaemic periodic paralysis type 2 caused by mutations at codon 672 in the muscle sodium channel gene SCN4A. *Brain* 124:1091–1099.
9. Kullmann DM, Hanna MG (2002) Neurological disorders caused by inherited ion-channel mutations. *Lancet Neurology* 1:157–166.
10. Sokolov S, Scheuer T, Catterall WA (2007) Gating pore current in an inherited ion channelopathy. *Nature* 446:76–78.
11. Struyk AF, Cannon SC (2007) A Na^+ channel mutation linked to hypokalemic periodic paralysis exposes a proton-selective gating pore. *J Gen Physiol* 130:11–20.
12. Jurkat-Rott K, Lehmann-Horn F (2007) Do hyperpolarization-induced proton currents contribute to the pathogenesis of hypokalemic periodic paralysis, a voltage sensor channelopathy? *J Gen Physiol* 130:1–5.
13. Senatorov VV, Stys PK, Hu B (2000) Regulation of Na+,K+-ATPase by persistent sodium accumulation in adult rat thalamic neurones. *J Physiol* 525:343–353.
14. Hirn C, Shapovalov G, Petermann O, Roulet E, Ruegg UT (2008) Nav1.4 deregulation in dystrophic skeletal muscle leads to Na+ overload and enhanced cell death. *J Gen Physiol* 132:199–208.
15. Nielles-Vallespin S, *et al.* (2007) 3D radial projection technique with ultrashort echo times for sodium MRI: Clinical applications in human brain and skeletal muscle. *Magn Reson Med* 57:74–81.
16. Neher E, Sandblom J, Eisenman G (1978) Ionic selectivity, saturation, and block in gramicidin A channels. II. Saturation behavior of single channel conductances and evidence for the existence of multiple binding sites in the channel. *J Membr Biol* 40:97–116.
17. Dyck PJ, *et al.* (2005) History of standard scoring, notation, and summation of neuromuscular signs. A current survey and recommendation. *Journal of the Peripheral Nervous System* 10:158–173.
18. Tricarico D, Barbieri M, Camerino DC (2000) Acetazolamide opens the muscular KCa2+ channel: A novel mechanism of action that may explain the therapeutic effect of the drug in hypokalemic periodic paralysis. *Ann Neurol* 48:304–312.
19. Tricarico D, *et al.* (2008) Acetazolamide prevents vacuolar myopathy in skeletal muscle of K(+)-depleted rats. *Br J Pharmacol* 154:183–190.
20. Blair NF, Krieger NS, Bushinsky D (1990) Mechanism of amphotericin B stimulation of net calcium efflux from neonatal mouse calvariae. *J Bone Miner Res* 5:725–732.
21. Plaster NM, *et al.* (2001) Mutations in Kir2.1 cause the developmental and episodic electrical phenotypes of Andersen's syndrome. *Cell* 105:511–519.
22. Struyk AF, Cannon SC (2008) Paradoxical depolarization of Ba2+-treated muscle exposed to low extracellular K+: Insights into resting potential abnormalities in hypokalemic paralysis. *Muscle Nerve* 37:326–337.
23. Azuma KK, Hensley CB, Putnam DS, McDonough AA (1991) Hypokalemia decreases Na(+)-K(+)-ATPase alpha 2-but not alpha 1-isoform abundance in heart, muscle, and brain. *Am J Physiol* 260:C958–964.
24. Griggs RC, Engel WK, Resnick JS (1970) Acetazolamide treatment of hypokalemic periodic paralysis. Prevention of attacks and improvement of persistent weakness. *Ann Intern Med* 73:39–48.
25. Marden FA, Connolly AM, Siegel MJ, Rubin DA (2005) Compositional analysis of muscle in boys with Duchenne muscular dystrophy using MR imaging. *Skeletal Radiology* 34:140–148.
26. Raab-Graham KF, Radeke CM, Vandenberg CA (1994) Molecular cloning and expression of a human heart inward rectifier potassium channel. *NeuroReport* 5:2501–2505.
27. Bakowski D, Parekh AB (2007) Voltage-dependent Ba2+ permeation through store-operated CRAC channels: Implications for channel selectivity. *Cell Calcium* 42:333–339.
28. Ouwerkerk R, *et al.* (2008) Tissue sodium concentration in myocardial infarction in humans: A quantitative ^{23}Na MR imaging study. *Radiology (Easton, Pa)* 248:88–96.
29. Chahine M, *et al.* (2005) NHE-1-dependent intracellular sodium overload in hypertrophic hereditary cardiomyopathy: Prevention by NHE-1 inhibitor. *J Mol Cell Cardiol* 38:571–582.
30. Estrada M, Liberona JL, Miranda M, Jaimovich E (2000) Aldosterone- and testosterone-mediated intracellular calcium response in skeletal muscle cell cultures. *Am J Physiol Endocrinol Metab* 279:E132–139.
31. Macdonald JE, Struthers AD (2004) What is the optimal serum potassium level in cardiovascular patients? *J Am Coll Cardiol* 43:155–161..